

Buckling Loads and Effective Length Factor for Non-Prismatic Columns

Taghreed Hassan Ibrahim

Assistant Lecture

Department of Civil Engineering

College of Engineering-University of Baghdad

E-mail: tegreed@yahoo.com

ABSTRACT

Based on a finite element analysis using Matlab coding, eigenvalue problem has been formulated and solved for the buckling analysis of non-prismatic columns. Different numbers of elements per column length have been used to assess the rate of convergence for the model. Then the proposed model has been used to determine the critical buckling load factor (γ_{cr}) for the idealized supported columns based on the comparison of their buckling loads with the corresponding hinge supported columns. Finally in this study the critical buckling factor (γ_{cr}) under end force (P) increases by about 3.71% with the tapered ratio increment of 10% for different end supported columns and the relationship between normalized critical load and slenderness ratio was generalized.

Keywords: Buckling load, non-prismatic, finite element, eigenvalue.

أحمال الانبعاج ومعامل الطول الفعال للأعمدة غير المنشورية

تغريد حسن إبراهيم

مدرس مساعد

قسم الهندسة المدنية

كلية الهندسة - جامعة بغداد

الخلاصة

بالاعتماد على نظرية تحليل العناصر المحددة وباستخدام برنامج الماتلاب تمت صياغة مشكلة القيمة الذاتية وحلها وفقا لتحليل الانبعاج للأعمدة غير المنشورية. تم استخدام أعداد مختلفة من العناصر على امتداد طول العمود لتقييم معدل التقارب للنموذج الأمثل. لقد تم استخدام النموذج المقترح لتحديد معامل الانبعاج الحرج (γ_{cr}) لأعمدة مثالية الإسناد وذلك للمقارنة بين أحمال الانبعاج لحالات إسناد مختلفة للأعمدة مع حالة الإسناد البسيط. وأخيرا كانت الزيادة لمعامل الانبعاج الحرج (γ_{cr}) بحدود 3,71% لكل 10% زيادة في نسبة التدبب لمختلف حالات الإسناد وكذلك تم تعميم العلاقة بين الحمل الحرج ونسبة النحافة للأعمدة.

الكلمات الرئيسية: حمل الانبعاج، غير منشوري، العناصر غير المحددة، القيمة الذاتية.

1. INTRODUCTION

Determination of critical buckling load for elastic column is a key problem in engineering design. Non-prismatic or tapered compression members are often used to achieve economy in many practical applications, **Shengmin, 1996**. The first study on elastic stability is attributed to **Euler, 1744**, who used the theory of calculus of variations to obtain the equilibrium equation and buckling load of a compressed elastic column. Since many studies in this field have been made such as **Gere, et al., 1962**, derived exact buckling solutions for many types of tapered columns with simple boundary conditions. **Ermopoulos, 1986** studied the buckling of the tapered columns under axially concentrated loads at any position along the length direction for the parabolically varying bending stiffness, **Gere, et al., 1962**. **Groper, et al., 1987**, developed a method for predicting the critical buckling load for the particular case of concentrically loaded

columns with variations in cross-sectional area. **Rzaiee, et al., 1995**, used a geometrical nonlinear analysis to solve non-prismatic or nonsymmetrical thin walled I-beam or columns, and by using a computer program they generalized the results in form of design tables. **Shengmin, 1996**, used a modified matrix technique to study the elastic and inelastic buckling capacity of non-prismatic members with a linear tapered I-shaped with a constant flange and a variable web. **Yossif, 2008**, derived the elastic critical load of a non-prismatic member using the equations of the modified stability functions for a wide range of taper ratio for rectangular or square cross sectional shapes. **Wei, et al., 2010**, analyzed the buckling of prismatic and non-prismatic rectangular columns under its weight and external axial force and discussed the influence of the taper ratio on the critical buckling load. **Al-Sadder, et al., 2004**, determined an exact secant stiffness matrix for a fixed-end forces vector for non-prismatic beam-column members under tension and compression axial force.

2. THEORY

In the displacement field approach, a structure is usually dividing into a number of finite elements and these elements are interconnecting at joints termed nodes as shown in **Fig. 1**. The displacements within each element are represented by simple functions. The displacement function is generally expressed in terms of a polynomial to be as or trigonometric function. For a one dimensional idealization structure, the displacement field can be assumed in Eq. (1)[4]:

$$v(x) = a_1 + a_2x + a_3x^2 + a_4x^3 \quad (1)$$

where:

$v(x)$: Is the displacement function at any x along the element.

a_1, a_2, a_3 and a_4 : Is the coefficients of the generalized coordinates.

In a matrix form, $v(x)$ can be represented as;

$$v = \begin{bmatrix} 1 & x & x^2 & x^3 \end{bmatrix} \begin{bmatrix} a_1 \\ a_2 \\ a_3 \\ a_4 \end{bmatrix} \quad (2)$$

The relation between the nodal degrees of freedom and the generalized coordinates can be expressed in Eq.(3):

$$v = [x]\{a\} \quad (3)$$

and

$$\theta = v' = \begin{bmatrix} 0 & 1 & 2x & 3x^2 \end{bmatrix} \begin{bmatrix} a_1 \\ a_2 \\ a_3 \\ a_4 \end{bmatrix} \quad (4)$$

Hence ; nodal displacements of an individual element will be expressed as:

$$[d] = \begin{bmatrix} v_1 \\ \theta_1 \\ v_2 \\ \theta_2 \end{bmatrix} = \begin{bmatrix} 1 & 0 & 0 & 0 \\ 0 & 1 & 0 & 0 \\ 1 & L & L^2 & L^3 \\ 0 & 1 & 2L & 3L^2 \end{bmatrix} \begin{bmatrix} a_1 \\ a_2 \\ a_3 \\ a_4 \end{bmatrix}$$

or

$$[d] = [A]\{a\} \tag{5}$$

then

$$\{a\} = [A]^{-1}\{d\} \tag{6}$$

Substitute Eq.(6) into Eq.(3) to get:

$$v = [x][A]^{-1}\{d\} \tag{7}$$

Where:

$$A^{-1} = \begin{bmatrix} 1 & 0 & 0 & 0 \\ 0 & 1 & 0 & 0 \\ \frac{-3}{L^2} & \frac{-2}{L} & \frac{3}{L^2} & \frac{-1}{L} \\ \frac{2}{L^3} & \frac{1}{L^2} & \frac{-2}{L^3} & \frac{1}{L^2} \end{bmatrix} \tag{8}$$

The total potential energy (Π_p) for a member that subjected to an axial force (P) is expressed in Eq. (9):

Π_p = strain energy + potential energy of applied force [2]

$$\Pi_p = \int_0^L \frac{EI}{2} \left(\frac{d^2v}{dx^2} \right)^2 dx + \int_0^L \frac{P}{2} \left(\frac{dv}{dx} \right)^2 dx \tag{9}$$

This equivalent assumed that the potential of the loads is considered to be due to the forces normal to the column length only. The summation of the two integrals of Eq. (9) is considered as $\Pi_p=0$. [4]

The term $\left(\frac{dv}{dx} \right)^2 / 2$ in the second integral expresses the strain due to rotation of the beam element a length of $(dx \left(\frac{ds-dx}{dx} \right))$.

$$\frac{ds-dx}{dx} = \frac{(dx^2+dv^2)^{1/2}-dx}{dx} = [1 + (v')^2]^{1/2} - 1 \approx \frac{(v')^2}{2}$$

Based on the above statements:

$$\Pi_p = \int_0^L \frac{EI}{2} v_{,xx}^2 dx + \int_0^L \frac{P}{2} v_{,x}^2 dx \tag{10}$$

Where: $v_{,xx} = \frac{d^2v}{dx^2}$, $v_{,x} = \frac{dv}{dx}$

From Eq.(7) it will be get:

$$v_{,xx} = [x''] [A]^{-1} \{d\} \tag{11}$$

And noting that , $v_{,xx}^2 = [v_{,xx}]^T [v_{,xx}]$

$$v_{,xx} = [B] \cdot \{d\} \tag{12}$$

Where:

$$[B] = [x''] \cdot [A]^{-1}$$

$$\begin{aligned} \Pi_p = & \frac{EI}{2} \int_0^L \{d\}_{1 \times 4}^T \cdot [B]_{4 \times 1}^T \cdot [B]_{1 \times 4} \{d\}_{4 \times 1} \cdot dx \\ & + \frac{P}{2} \int_0^L \{d\}^T \cdot [A]^{-T} \cdot [x']^{-T} \cdot [x'] \cdot [A]^{-1} \cdot \{d\} dx \end{aligned} \tag{13}$$

For a compressive force (P), we have $\Pi_p = \frac{1}{2} \{d\}^T [K] \{d\} - \frac{1}{2} \{d\}^T P [K_g] \{d\}$

Let $[K_e] = [K] - [K_g]$ =Equivalent stiffness matrix for a beam element of combined axial and a bending force actions.

Where:

$$[K] = \int_0^L [B]^T \cdot EI \cdot [B] dx \tag{14}$$

$[K_g]$ =Geometric stiffness matrix

$$[K_g] = P [\bar{k}]$$

$$[K_g] = P \int_0^L [A]^{-T} \cdot [x']^{-T} \cdot [x'] \cdot [A]^{-1} \cdot \{d\} dx \tag{15}$$

$$[K_g] = \frac{P}{30L} \begin{bmatrix} 36 & 3L & -36 & 3L \\ 3L & 4L^2 & -3L & -L^2 \\ -36 & -3L & 36 & -3L \\ 3L & -L^2 & -3L & 4L^2 \end{bmatrix} \tag{16}$$

The geometric stiffness matrix $[K_g]$ can be obtained by the consistent geometric stiffness technique and the main advantage of this method that the eigenvalues were more accurate and were proven upper bounds to the exact solution.

For the non-prismatic or tapered member we derived equation for the moment of inertia (I_x) of the section at any distance (x) from the smallest end can be expressed in Eq. (17):

$$I_x = I_o + (\lambda - 1)I_o \frac{x}{L} \quad (17)$$

Where:

I_o : Is the moment of inertia for the smallest section at $x=0$.

λ : Is the tapered ratio that represents the increasing in the moment of inertia so it's defined as the ratio of the moment of inertia at the bottom of the column I-section (I_L) to the moment of inertia at the top of the column I-section (I_o) as shown in **Fig. 2**.

Substitutes Eq. (17) into Eq. (14) and analytical integrated by Matlab software, an implicit form has been derived for stiffness matrix $[K]$.

Finally:

$$[[K] - [K_g]] \cdot \{D\} = \{F\} \quad (18)$$

For buckling problems: $\{F\} = \{0\}$, $\{D\} \neq \{0\}$ then

$$\det|K - K_g| = 0$$

Eigenvalue problems were solved by using the finite element method written in Matlab program. The program used the element stiffness, mass matrix and modified the eigenvalue matrix equation with given constraints. The modified eigenvalue matrix equation contained fictitious zero eigenvalues in the same number of constraints. Finally solved this eigenvalue problem and determine the critical buckling load factor (γ_{cr}) for the lowest eigenvalue. The critical buckling load is expressed as shown in Eq. (19):

$$P_{cr} = \gamma_{cr} \frac{\pi^2 EI}{L^2} \quad (19)$$

3. CASE STUDIES:

A tapered I-section column of a constant flange width and linear increasing in the web depth was adopted. It has a total length of (L) and under the effect of a concentrated axial load (P) on its top as shown in **Fig. 3**.

For the columns shown in **Fig. 3** there were different taper ratios (λ) of (1,1.1, 1.2, 1.3, 1.4, 1.5, 1.6, 1.7, 1.8, 1.9 and 2) with different boundary conditions of the hinged-hinged, clamped-free, clamped-hinged and clamped-clamped end supported columns have been considered. Critical buckling load factor (γ_{cr}) for the case studies has been summarized in **Table 1**.

The following notations were used to describe column boundary conditions for different end supports are summarized in **Table 2**.

4. VERIFICATION:

In order to investigate the validity of the results of the program we had to compare the buckling load factor for linear tapered I-sections column for the tapered ratio of one only because of the difference in the calculation of the studies for the tapered ratio where, **Wei,2010**, and **Yossif, 2008**, considered the tapered ratio as the ratio of width to length of a rectangular column section,

while in this study the tapered ratio is considered as the ratio of the moment of inertia at the bottom to the top of the I-section, since the verification is used tapered ratio of one only and the result was almost identical as shown in **Table 3**.

5. RESULTS AND DISCUSSIONS:

By using the finite element method in Matlab program to solve the eigenvalue problem in order to compute the critical buckling load factor for the non-prismatic or tapered I-shape steel column member, with linearly varied web height and with constant flange dimension.

Table 1 gave the critical buckling load factor (γ_{cr}) of the web tapered column under axial force (P) acting at the top of the column for different boundary conditions. Different number of elements (from 4 to 11) along column length gave results that are quite close with a relative error not greater than (3%).

The results obtained from **Table 1** showed that average increasing in tapered ratio leads to increasing the buckling load factor about 4.17% for the hinged-hinged end supported column and about 3.6% for the clamped-free, clamped-hinged and clamped-clamped end supported columns, that mean for each 10% increase in the moment of inertia for the column section leads to average increasing of 3.71% for the hinged-hinged, clamped-free, clamped-hinged and clamped-clamped end supported columns.

To present the relationship between the normalized critical load defined by $(P_{cr}/f_y.A)$ and the slenderness ratio (KL/r) as shown in **Table 4** and **Fig. 4**, the hinged-hinged column end supports was implemented with different tapered ratios of (1, 1.2, 1.4, 1.6, 1.8 and 2) and used the wide-flange section of (W30x211) as shown in **Table 5** to represents the section properties of the radius of gyration (r), moment of inertia (I), and area of the section (A). The modulus of elasticity (E) and the yield strength of steel (f_y) were considered as (200 GPa) and (250 MPa) respectively. The slenderness ratio was limited by the maximum short and intermediate column limit (C_c) factor which calculate from the Eq.(20) and the maximum long column limit $(KL/r=200)$ [6].

$$C_c = \sqrt{\frac{2\pi^2 E}{f_y}} \quad (20)$$

Convergence for the critical buckling factor for the case of hinged-hinged column end supports could be obtained with three or more elements mesh as shown in **Fig. 5**.

6. CONCLUSIONS:

- The buckling of non-prismatic columns or tapered I-shaped steel column under tip force was analyzed by finite element method using Matlab coding.
- The boundary condition at both ends of column were processed in the program for the hinged-hinged, clamped-free, clamped-hinged and clamped-clamped end supported columns.



- The lowest eigenvalue gave the desired buckling load factor for different tapered ratios (λ) of (1,1.1, 1.2, 1.3, 1.4, 1.5, 1.6, 1.7, 1.8, 1.9 and 2) .
- The critical buckling factor (\mathbf{Y}_{cr}) under end force (P) increases by about 3.71% with the tapered ratio increment of 10% for different end supported columns..
- Relationship between normalized critical load and limited slenderness ratio was generalized.
- For the hinged-hinged supports, from (3-7) elements along the column length obtained a fair convergence for the model for this study.

REFERENCES:

- Al-Sadder, S. Z., and Qasrawi, 2004, *Exact Secant Stiffness Matrix for Nonprismatic Beam-Columns with Elastic Semi rigid Joint Connections*, Emirates Journal for Engineering Research, Vol. 9, No.2, PP.127-135.
- Chandraupatla, T. R., and Belegunu, A. D., 1990, *Introduction to Finite Elements in Engineering*, U.S.A.
- Groper, M. and Kenig, M. J., 1987, *Inelastic Buckling of Non-prismatic Columns*, Journal of Engineering Mechanics, Vol.113, No.8, August, PP. 263-279.
- Iyengar , N. G. R., 1986, *Structural Stability Of Columns And Plates*, Affiliated East-West Press, New Delhi.
- Rzaiee-Pajand, M. and Moayedian, M., 1995, *Nonprismatic Beam and Column Design Table for Nonlinear Analysis*, Asian Journal of Structural Engineering, Vol.1, No.4, PP. 337-349.
- Shengmin, B. Wu., 1996, *Inelastic Buckling Loads for Nonprismatic Columns*, The Journal of Chaoyang, University of Technology Vol.6, No. 1, PP. 263-279.
- Timoshenko, S., and Gere, J. M., 1961, *Theory of Elastic Stability*, 2nd Edition, New York.
- Wei, D. J., Yan, S. X., Zhang, Li X.-F., 2010, *Critical Load for Buckling of Non-Prismatic Columns Under Self-Weight and Tip Force*, Mechanics Research Communications, Vol. 37, PP. 554–558.
- Yossif, W. V., 2008, *Elastic Critical Load of Tapered Members*, Journal of Engineering and Development, Vol. 12, No.1, PP. 148-160.
- Young, W. Kwan, Hyocoong Bang, 2000, *The Finite Element Method Using MATLAB*, 2nd Edition, New York.

NOMENCLATURE:

L = is the column length.

P = is the axial load.

P_{cr} = is the critical buckling load.

γ_{cr} = is the critical buckling factor.

λ = is the taper ratio.

r = is the radius of gyration.

A = is the area of column section.

I = is the moment of inertia.

I_x = is the moment of inertia for the section of the tapered member at any distance (x)

I_o = is the moment of inertia for the smallest section of the tapered member at $x=0$.

I_L = is the moment of inertia at the top of the column I-section.

E = is the steel modulus of elasticity

f_y = is the yield strength of steel.

C_c = is represents the theoretical demarcation line between inelastic and elastic behavior.

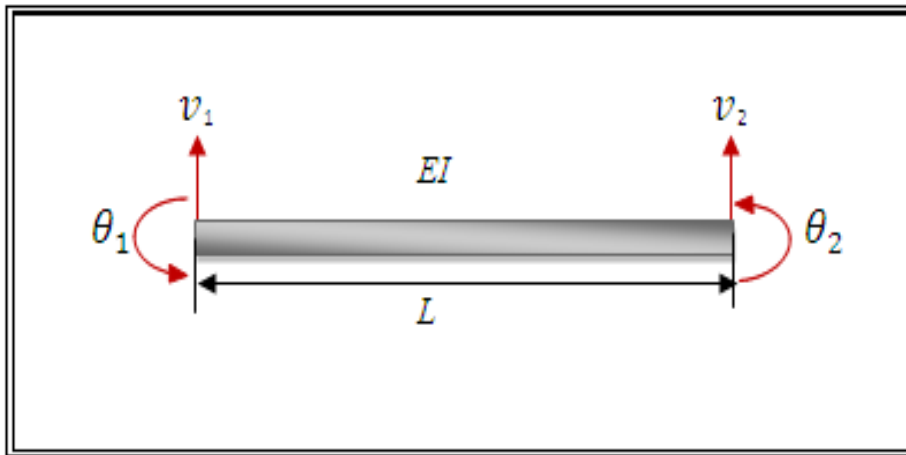


Figure 1. Beam Element.

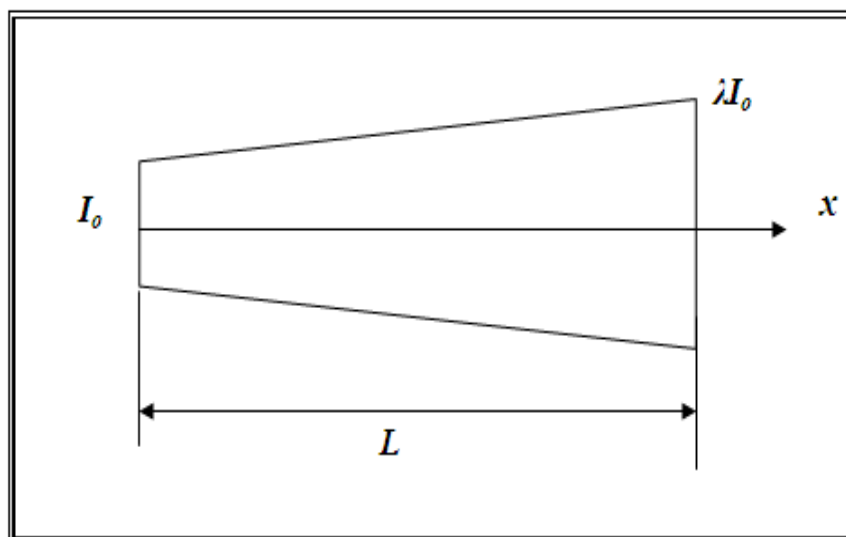


Figure 2. Tapered ratio of non-prismatic column member.

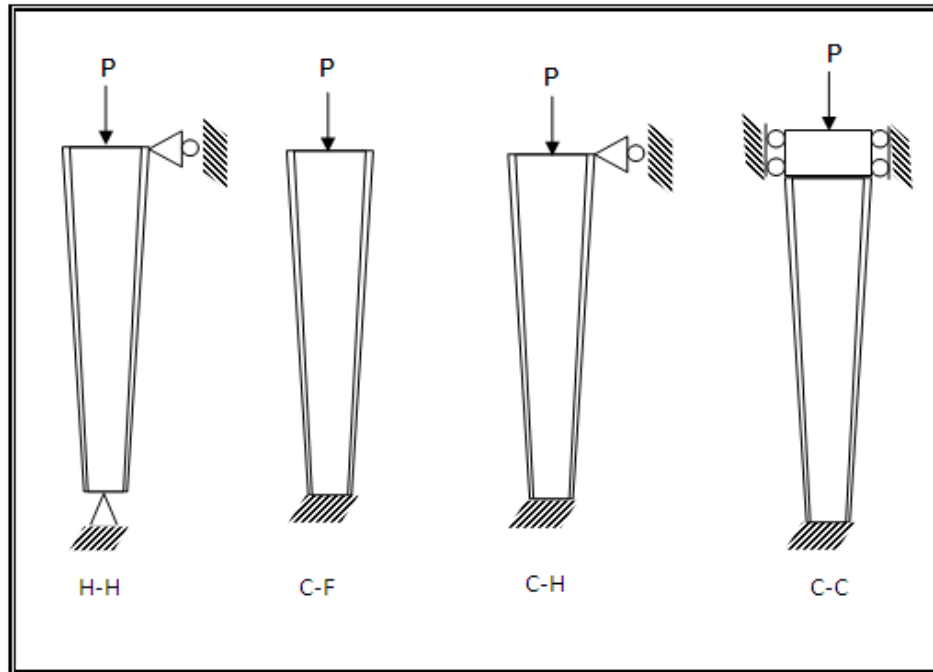


Figure 3. Schematic of tapered I-sections columns under tip force with different boundary conditions.

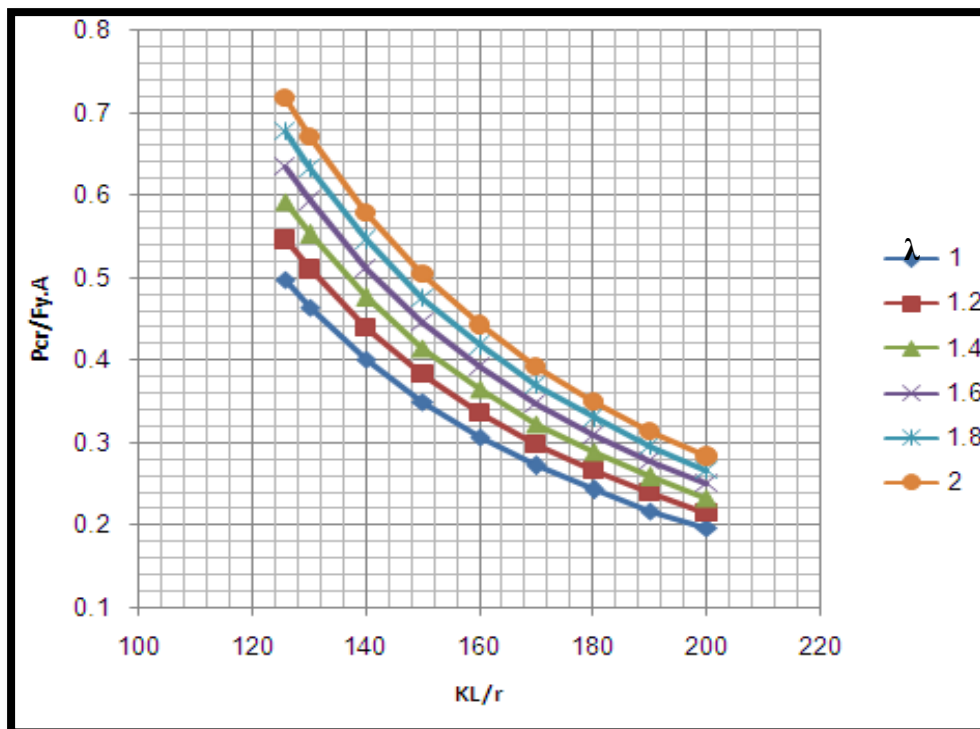


Figure 4. The normalized critical load verses the slenderness ratio.

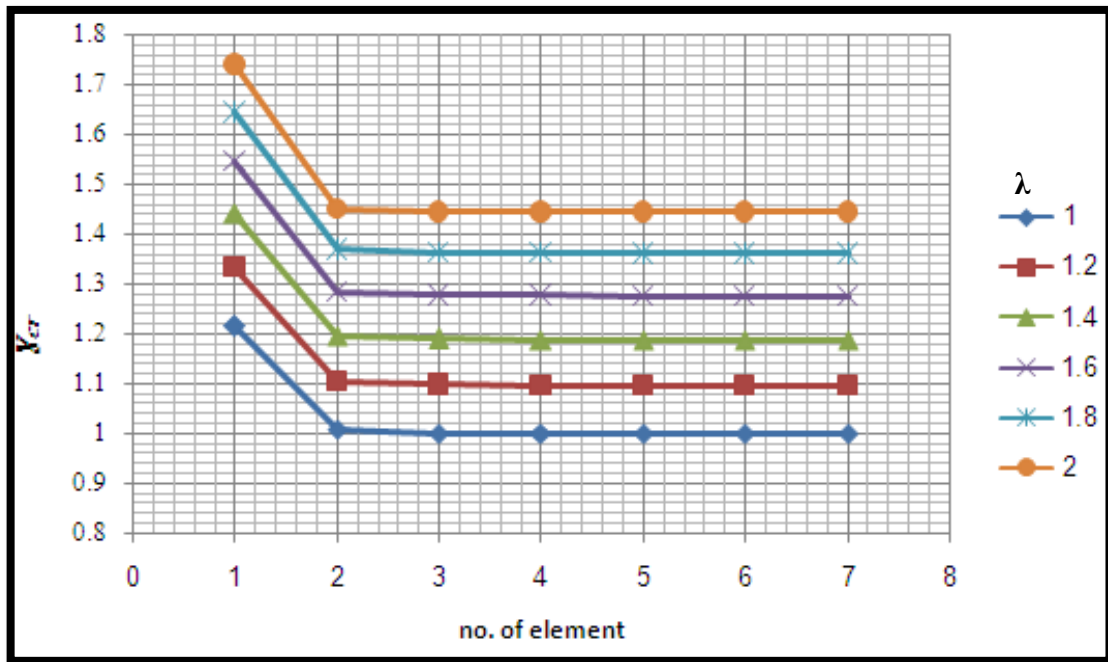


Figure 5. Relationship between the number of elements and the critical buckling factor for the hinged-hinged column end supports.

Table 1. The Critical Buckling Factor with Variable Tapered Ratio.

λ	(Y_{cr}) for H-H	No. of Element	(Y_{cr}) for C-F	No. of Element	(Y_{cr}) for C-H	No. of Element	(Y_{cr}) for C-C	No. of Element
1	1.000056	7	0.249999	7	2.046172	7	4.001155	9
1.1	1.049277	7	0.261711	8	2.140907	4	4.19873	8
1.2	1.097101	6	0.272958	7	2.237161	10	4.39124	7
1.3	1.143516	7	0.284103	7	2.324297	7	4.575643	9
1.4	1.188897	7	0.294864	7	2.416499	9	4.758021	7
1.5	1.233377	7	0.306293	10	2.501608	8	4.936345	7
1.6	1.276945	7	0.315715	7	2.582665	7	5.110617	7
1.7	1.361852	7	0.325847	7	2.669801	8	5.281849	7
1.8	1.403363	7	0.337499	10	2.755923	9	5.450041	7
1.9	1.403393	7	0.34753	11	2.841033	10	5.615194	7
2	1.444327	7	0.357459	11	2.925129	11	5.779029	7



Table 2. The Column Boundary Conditions of The Different End Supports.

Type of The Column End Supports	Boundary Conditions
(Hinged-Hinged) columns (H-H)	@x=0, v=0 @x=L, v=0
(Clamped-Free) columns (C-F)	@x=0, v=0 @x=0, $\theta=0$
(Clamped-Hinged) columns (C-H)	@x=0, v=0 @x=0, $\theta=0$ @x=L, v=0
(Clamped-Clamped) columns (C-C)	@x=0, v=0, @x=0, $\theta=0$ @x=L, v=0, @x=L, $\theta=0$

Table 3. Verification of the Critical Buckling Factor with Tapered Ratio(λ)=1.

Type of the Column End Supports	(γ_{cr}) _{present study}	(γ_{cr}) _{Wie. 2010[8]}	(γ_{cr}) _{Yossif.2008[9]}
(Hinged-Hinged) columns (H-H)	1.000056	1.0000401	1.000000
(Clamped-Free) columns (C-F)	0.249999	0.2499594	0.250000
(Clamped-Hinged) columns (C-H)	2.046172	2.045776	2.045752
(Clamped-Clamped) columns (C-C)	4.001155	3.999957	-

Table 4. The Non-dimensional Critical Load with Slenderness Ratio for the wide-flange section of (W30x211).

KL/r	$P_{cr}/f_y \cdot A$ $\lambda=1$	$P_{cr}/f_y \cdot A$ $\lambda=1.2$	$P_{cr}/f_y \cdot A$ $\lambda=1.4$	$P_{cr}/f_y \cdot A$ $\lambda=1.6$	$P_{cr}/f_y \cdot A$ $\lambda=1.8$	$P_{cr}/f_y \cdot A$ $\lambda=2$
125.66	0.4973	0.5456	0.5912	0.6349	0.6771	0.7181
130	0.4646	0.5007	0.5523	0.5932	0.6326	0.6709
140	0.4006	0.4395	0.4762	0.5115	0.5455	0.5785
150	0.3489	0.3827	0.4148	0.4455	0.4751	0.5039
160	0.3067	0.3365	0.3646	0.3916	0.4176	0.4429
170	0.2717	0.2981	0.323	0.3469	0.3699	0.3923
180	0.2423	0.2658	0.288	0.3093	0.3299	0.3499
190	0.2175	0.2386	0.2585	0.2776	0.296	0.314
200	0.196	0.215	0.233	0.2502	0.2668	0.283

Table 5. The Properties of Wide-Flange Section (W30x211).

Designation	Area (mm ²)	Web thickness(mm)	$I \times 10^6$ (mm ⁴)	r(mm)
W30x211	40100	19.7	4290	328